Selective CO_2 Hydrogenation to Formic Acid with Multifunctional Ionic Liquids

Andreas Weilhard, [‡¥] Muhammad I. Qadir, [†] Victor Sans, [*‡¥] and Jairton Dupont[*‡†]

[‡]GSK Carbon Neutral Laboratories for Sustainable Chemistry–NG7 2GA, University of Nottingham, UK

[†]Institute of Chemistry–UFRGS–Av. Bento Gonçalves, 9500, Porto Alegre, 91501-970, RS, Brazil

[¥]Faculty of Engineering, University of Nottingham, NG7 2RD, Nottingham, UK.

ABSTRACT: The development of simple, cost-effective and sustainable methods to transform CO_2 into feedstock chemicals is essential to reduce the dependence on fossil fuels of the chemical industry. Here, we report the selective and efficient catalytic hydrogenation of CO_2 to formic acid (FA) using a synergistic combination of an ionic liquid (IL) with basic anions and relatively simple catalysts derived from the precursor $[Ru_3(CO)_{12}]$. Very high values of TON (17000) and TOF have been observed and FA solutions with concentrations of up to 1.2 M have been produced. In this system, the imidazolium based IL associated with the acetate anion acts as precursor for the formation of the catalytically active Ru-H species, catalyst stabilizer and as an acid buffer, shifting the equilibrium towards free formic acid. Moreover, the IL acts as an entropic driver (via augmentation of the number of microstates), lowering the entropic contribution imposed by the IL surrounding the catalytically active sites. The favorable thermodynamic conditions enable the reaction to proceed efficiently at low pressure pressures, and furthermore the immobilization of the IL onto a solid support facilitates the separation of FA at the end of the reaction.

Introduction

Formic acid (FA) is a primary product of the chemical industry with a production capacity of 600,000 tons per year and a projected annual increase of 22%.[1] Most commonly formic acid is synthesized by MeOH carbonylation, yielding a formate ester which is then hydrolyzed with an excess of water.[2] The transformation of CO_2 to FA in one step using H_2 from renewable sources represents a more sustainable alternative to the current synthesis, being less resource intensive, using an abundant resource (CO_2) and by avoiding the generation of intermediates and the need for tedious purifications. Furthermore, the direct synthesis of formic acid from CO_2 potentially represents a vector for hydrogen storage.[3-5] Unfortunately, this transformation is hugely challenging due to the inherent kinetic and thermodynamic stability of CO_2.[6-7] One strategy which has been used frequently to overcome thermodynamic limitations is the use of suitable bases.[8] Under these conditions, a plethora of catalysts based on N-heterocyclic-carbenes[9-10], half-sandwich compounds[3, 11-12], pincer ligands[13-16] and phosphines[8, 17-20], combined with noble metals such as Ir, Ru and Rh have been described and reported, in some cases, to display very high TON and TOF values.[13] A key consideration in these systems is the synthesis of stable formate adducts or salts, requiring tedious purifications to separate the formic acid.[6, 21-23]

An ideal scenario would involve the direct formation of formic acid in base free systems or systems with weak bases, where the FA could be readily recovered. Due to the above mentioned limitations, such systems are rather scarce (see SI Table S1 for a summary of results and values of TON and TOF).[24, 26] Formate buffers have been introduced to stabilize the catalyst in the acidic aqueous media, thus increasing the achievable concentration of formic acid with moderate success (up to a final concentration of 0.11M).[27] Alternatively, the employment of DMSO/water mixtures yielded high

formic acid concentrations, although the catalytic activity was relatively low.[28] In 2016, Leitner and co-workers reported a Ru(triphos)-catalyst which achieved high TON and TOF in the presence of sodium acetate (NaOAc).[29]

Ionic liquids (ILs) are very interesting media for the transformation of carbon dioxide, due to its high solubility in solutions of IL and aqueous or organic solvents with significant aqueous content.[30a] This is particularly important in those ILs based on imidazolium cations which are associated with basic anions such as acetate, due to the formation of bicarbonate and the acid buffering properties of these solutions.[30b]
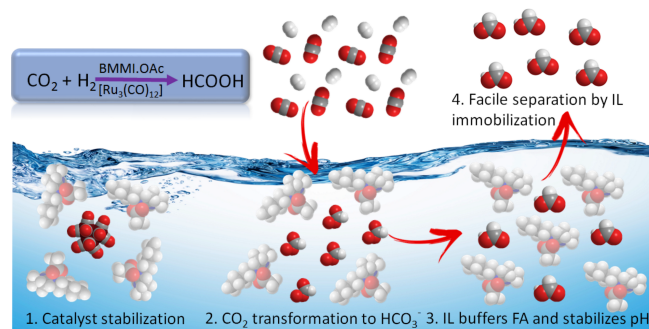
Figure 1. Multiple roles performed by ILs in the selective and efficient hydrogenation of CO_2 to formic acid (FA). Basic ILs are shown to: 1. stabilize the catalyst; 2. facilitate formation of bicarbonate in the presence of water; 3. buffer the reaction media and; 4. facilitate the isolation of FA from the reaction upon immobilization of the IL followed by simple filtration.

ILs with basic anions, such as 1,3-Propyl-2-methylimidazolium formate (PPMI.O_2CH), enhance the yield of the reaction by thermodynamically favoring product formation.[31] Indeed, in this system, a change in enthalpy of -20 kJ mol^{-1} was observed, being higher than in conventional organic solvents and water, but lower than that when formate adducts are formed. Consequently, a scaled-up process would have to overcome a lower energy barrier, e.g. reactive distillation is not necessary to form formic acid from formate adducts during product isolation.[31] Furthermore, high activity (TOF = 300 h^{-1}) in presence of 3-propyl-1,2-dimidazolium formate (PMMI.O_2CH) has been reported, although the extraction efficiency of FA from the IL into the apolar $scCO_2$ phase reached only 10% after >60 h.[32]

Here, we present a remarkably active and selective catalytic system, where basic ILs perform multiple roles in the direct hydrogenation of CO_2 to formic acid using a Ru-catalyst (Figure 1). The ILs play a key role in the stabilization of the catalyst, assist the transformation of CO_2 into bicarbonate and buffers the system, shifting the equilibrium towards production of formic acid.

Results and Discussion

Hydrogenation of CO_2 to formic acid

Firstly, the role of a series of ILs were explored under reaction conditions usually employed for the hydrogenation of CO_2 to formic acid using ruthenium based catalyst precursors (Table 1).[4] Remarkably, when 1,2-dimethyl-3-butylimidazolium acetate (BMMI.OAc) was employed, very high turnover numbers (TON) were observed (up to 17000) with an average turnover frequency (TOF) of 102 h^{-1}. Under these conditions, a 1.1 M solution of FA was obtained (entry 6, table 1). An increased TOF of 300 h^{-1} was obtained at 80°C, though at the expense of a lower TON of 6875 (table 1, entry 8). Upon increasing the reaction time to 40 h, a TON of 8355 was reached at the cost of a lower TOF (200 h^{-1}) (table 1, entry 9). It is important to note that these very high TON and TOF values were achieved using a simple, cheap and commercially available [$Ru_3(CO)_{12}$] species as the pre-catalyst under substantially milder conditions than the state of the art for FA synthesis from CO_2 without the use of bases for formate stabilization.[28-29, 32] Table S1 shows a comparison with the best reported values in the literature.

The specific interaction of BMMI.OAc with the reaction media was demonstrated by exploring the same reaction using a series of ILs with different properties. In the first instance, no FA (or any other product) formation was observed without an IL (table 1, entry 1). This reveals that the IL has a vital role in the hydrogenation of CO_2 to FA based on its buffering properties and stabilization of weak carbonic acid species. The formation of FA is favorable under basic reaction conditions and therefore different basic ILs (BMMI.Cl and BMMI.Im) were also investigated (Table 1, entries 2 and 3). Surprisingly, no FA was observed when employing BMMI.Cl, which may be related to the IL poisoning the catalysts during CO_2 hydrogenation reactions.[26] Despite the theoretical buffering and basic properties of BMMI.Im, no catalytic activity was observed (Table 1, entry 3), possibly due to the ability of the imidazolate anion to bind to the catalytically active species, forming carbenes, thus competing with the CO_2 hydrogenation reaction. This would also be the case for other basic counteranions such as triazolate and therefore more detailed studies with other highly basic and possibly strongly coordinating ILs were dismissed. When BMMI.O_2CH was employed, relatively low activity for FA formation (TON = 55) was observed, as compared to BMMI.OAc (Table 1, entries 4, 11 and 12). This effect may be due to the lower pKa of the formate counter anion as compared to the acetate anion. The higher pH resulting from this buffering process prevents the protonation of Ru-H active species, thus keeping it in active state.[27,29, 33] Furthermore,

(N)Bu_4.OAc IL and NaOAc showed lower activities than BMMI.OAc, with TONs of 157 and 35.6, respectively (Table 1, entries 13-15,) after 4 h.

Table 1. Catalytic hydrogenation of CO_2 to FA by [$Ru_3(CO)_{12}$] catalyst at 60 °C.

$Me-N^+N\ ^nBu$ with R and X^-

R = Me, X = OAc, **BMMI.OAc**
R = Me, X = Cl, **BMMI.Cl**
R = Me, X = HCO_2, **BMMI.O_2CH**
R = Me, X = Imidazolate, **BMMI.Im**
R = H, X = OAc, **BMI.OAc**

Entry[a]	IL	t / h	[FA] / M	TON [d]	TOF[e] / h^{-1}
1	-	4	-	-	-
2	BMMI.Cl	4	-	-	-
3	BMMI.Im	4	-	-	-
4	BMMI.OAc	4	0.42	267.2	67
5	BMMI.OAc	72	1.10	700	9.7
6 [b]	BMMI.OAc	168	1.10	17,000	102.4
8 [c]	BMMI.OAc	20	0.43	6875	300
9 [c]	BMMI.OAc	40	0.52	8355	200
10	BMI.OAc	4	0.12	80	20
11	BMMI.O_2CH	4	0.09	55	13.8
12	BMMI.O_2CH	72	0.46	296	4.1
13	N(Bu)$_4$.OAc	4	0.24	157	39
14	N(Bu)$_4$.OAc	72	0.96	617	8.6
15	NaOAc	4	0.06	35.6	9

[a]Reaction conditions: Cat. (7.8 µmol), BMMI.OAc (0.66 M, 0.7 g), DMSO/H_2O (5 v/v%; DMSO (5.24 mL, 67 mmol), H_2O (0.24 mL, 13.2 mmol) and CO_2/H_2 (1:1, 40 bar). [b] Cat. (0.3 µmol), CO_2/H_2 (30 bar CO_2/40 bar H_2) and 70 °C. [c] Cat. (0.3 µmol), CO_2/H_2 (30 bar CO_2/30 bar H_2) and 80 °C. [d]Calculated as mol FA/ mol [$Ru_3(CO)_{12}$] using ^{1}H-NMR. [e] Calculated as TON/$t_{reaction}$.

An important feature of the ILs ability to stabilize the formation of formic acid is a broad solvent compatibility. Indeed, various organic solvents in combination with BMMI.OAc were employed for the hydrogenation of CO_2 to formic acid. The hydrogenation was found to occur in a range of solvents (see table 2) where a range of different product concentrations were observed, indicating that the solvent still plays a role in the reaction outcome. The highest concentration was obtained with DMSO in combination with 5 v/v% H_2O, in agreement with previous reports.[28, 29] Higher concentrations of water lead to decreased catalytic activity probably, due to the dissociation of the DMSO/H_2O clusters (see SI, Table S2).[29] In methyl-*tert*-butylether, 2-methyltetrahydrofuran and 1,4-Dioxane, a phase separation can be observed after the reaction is completed, where the IL, catalyst and FA are all dissolved in the same phase and the solvent has separated (Table 2, entry 4-6). This might be explained by the poor solubility of water and IL in these solvents.

Table 2. Solvent effect on FA concentration and catalytic activity observed.

Entry	Solvent[a]	Time[b] / h	[FA] / M	TON	TOF /h^{-1}

1	DMSO:H$_2$O	32	1.2	3609	106
2	THF:H$_2$O	18	0.7	2165	120
3	MeCN:H$_2$O	21	0.50	1567	78
4[c]	MtBE:H$_2$O	20	0.83	2578	128
5[c]	MeTHF:H$_2$O	18	0.66	2062	114
6[c]	Dioxane:H$_2$O	20	0.52	1629	81

Catalyst: [Ru$_3$(CO)$_{12}$] = 3.2*10^{-4}M; V$_{reaction}$= 5 mL; IL: BMMI.OAc; [IL]= 0.66M; P$_{H2}$=P$_{CO2}$= 30 bar; T = 60 °C. a) 5% v/v water b) Reaction time was adjusted until constant pressure observed. c) Biphasic mixture observed after the reaction.

Role of IL in the reaction mechanism and in stabilising the active catalytic species

The good results observed in terms of catalytic activity and selectivity under remarkably mild conditions encouraged us to investigate the reaction mechanism to understand the roles played by the ionic liquid. It has been previously shown that organic carbonates are readily hydrogenated to yield the corresponding formate esters.[34] Based on prior work[30] we hypothesized a bicyclic catalytic mechanism. In the first cycle, the IL catalyzes the formation of HCO$_3^-$ via "activated water" which is coordinated to BMMI.OAc in a similar way to that previously reported.[30] Indeed a signal of HCO$_3^-$ at 158 ppm was observed in the ^{13}C NMR, measured at relevant reaction conditions, of a mixture of IL, DMSO/H$_2$O and [Ru$_3$(CO)$_{12}$] (see Figure 2d). The carbonate formed *in-situ* then enters the second cycle, where it is hydrogenated by the Ru-hydride species to yield a formate complex, along with an associated elimination of water (Figure 2a). The signal assignable to catalyst-bound formic acid can be found at 166 ppm. Furthermore, a peak at 122 ppm assignable to CO$_2$ was observed (Figure 2d), confirming the proposed mechanism. A signal at 220 ppm corresponding to Ru-CO (see Figure S2), together with ESI-MS data (Figure 2e), indicate that the Ru cluster core is not transformed into monometallic species or Ru nanoparticles.

The amount of H$_2$O in the solvent was found to play a significant role (Table S2). An increasing amount of water seems to have a positive effect on the activity up to a 5% in volume. Afterwards, presumably the stabilization of the formic acid formed worsens due to the ineffective clustering of the buffer. The dissociation of H$_2$O was not involved in the rate-determining step, as opposed to previously reported mechanisms.[25, 26] This was determined by replacing H$_2$O with D$_2$O, leading to a secondary kinetic effect and a reduction in activity, i.e. the TOF decreased to 87 h^{-1} in the presence of D$_2$O versus 118 h^{-1} in the presence of H$_2$O (see SI Table S3 for more detail). One explanation for the secondary kinetic isotopic effect might be described by the formation of the carbonate prior to the rate determining step, thus giving further insight into the catalytic mechanism.

In this case, the rate determining step was found to be the regeneration of the active hydride species *via* abstraction of FA from the catalytic cycle with hydrogen. A TOF of 120 h^{-1} can be observed at a ratio of 2:1 (H$_2$/CO$_2$), which decreases almost in a linear fashion to 60 h^{-1} when the ratio of H$_2$ to CO$_2$ was lowered (Figure 2b). The hydrogenation step has been described previously as being rate determining with other Ru-catalysts.[25] An increase of the partial pressure of H$_2$ above a ratio of 2:1 compared to that of CO$_2$ showed no further increase in the reaction rate. This might be explained by the saturation of the liquid phase with H$_2$ in this regime, thus the limiting the effective concentration of H$_2$ available for the reaction.[35]

Formic acid can split from the metal center by either forming a bridged or terminal hydride. If a terminal hydride is formed this hydride would undergo isomerization to a bridged hydride regenerating the active species. In this regard, it is worth mentioning that bridged hydrides have been described as thermodynamically more stable.[36] Furthermore, trinuclear Ru-carbonyl-complexes with bridged acid ligands, similar to the proposed complex here have been described previously, thus being a more plausible mechanism.[37]
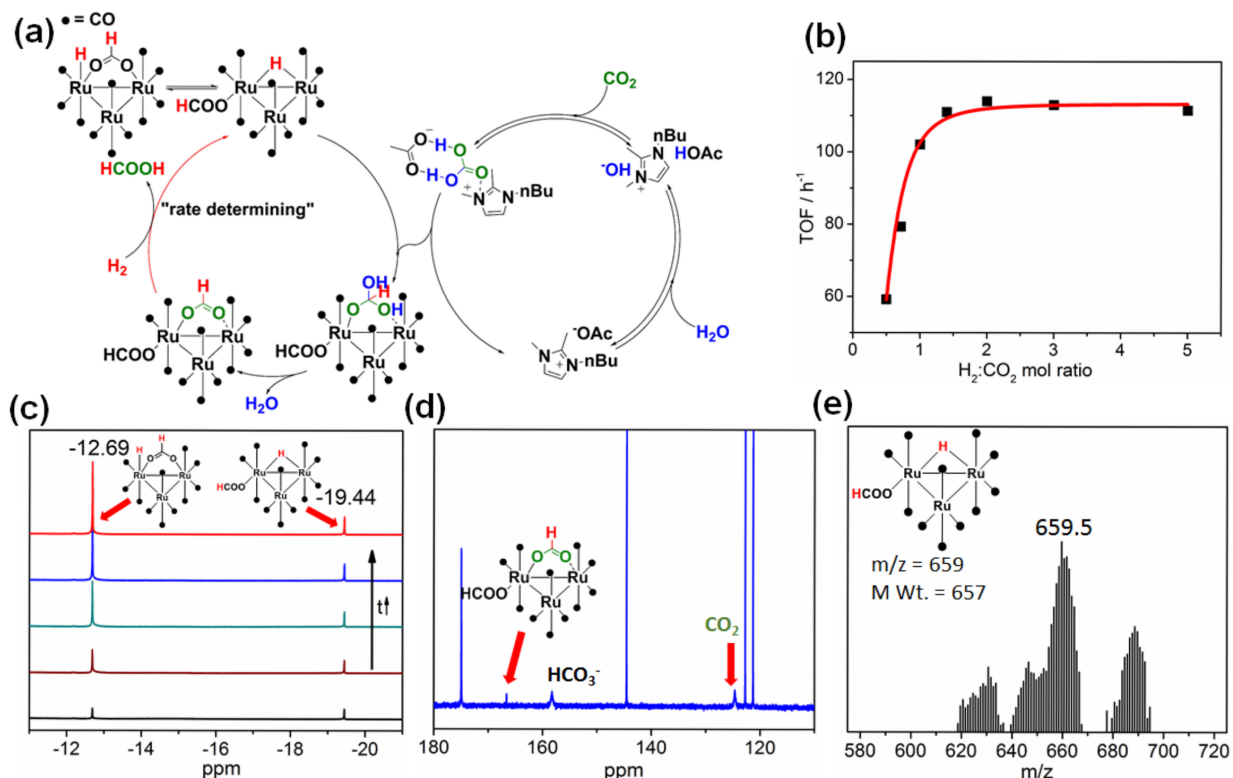
Figure 2. (a) proposed mechanism for CO_2 hydrogenation to FA. (b) TOF vs gas phase composition. Reaction conditions: total pressure= 60 bar, t = 4h, T = 60 °C, BMMI.OAc IL (0.66 M), $[Ru_3(CO)_{12}]$ = 7.8 µmol and DMSO/H_2O (5 v/v%; DMSO (5.24 mL, 67 mmol), H_2O (0.24 mL, 13.2 mmol). (c) High pressure ^{1}H-NMR and (d) High pressure ^{13}C-NMR spectra, both at P_{CO2} = P_{H2} = 20 bar, T = 25 °C with 23 µmol $[Ru_3(CO)_{12}]$ in DMSO/water with BMMI.OAc. (e) ESI-MS spectra of the $[Ru_3(CO)_{11}(H)(HCOO)]$ complex.

The IL is not only involved in the transformation of CO_2 to HCOOH but also assists the formation of the active species. Indeed, the active species are only observed in the presence of IL and H_2, indicating a co-operative mechanism involving the IL, water and hydrogen. The formation of the same hydride species were observed in the reaction mixture and in the in-situ high pressure ^{1}H NMR. The hydrides at -12.48 ppm and -19.48 ppm correspond to a terminal and to a bridging hydride respectively[38] (See Figure 2c and SI, Figure S1) akin to those already observed for dialkylimidazolium ILs with other anions.[39-40] Interestingly, a singlet at 8.48 ppm, corresponding to FA, can be detected even in the absence of CO_2, suggesting hydration of one CO-ligand, we suggest that the transformation of CO to HCOO takes place due to the interplay of $[Ru_3(CO)_{12}]$ with BMMI.OAc and H_2. In the ^{13}C NMR, the HCOO ligand from $[Ru_3(CO)_{11}(H)(HCOO)]$ was confirmed by observation of a peak at 164 ppm (see SI, Figure S2), analogous to that observed in Figure 2d. In addition, ESI-MS analysis revealed a peak at 659 m/z, corroborating the presence of $[Ru_3(CO)_{11}(H)(HCOO)]$ (see Figure 2e). No interaction between the BMMI.OAc IL and $[Ru_3(CO)_{12}]$ catalyst was observed by ^{13}C NMR spectroscopy. Moreover, when the catalyst was exposed to hydrogen in the absence of IL, the formate peak was not observed and the hydride peak previously observed at -19.48 ppm shifted to -17.16 ppm, indicating that a different hydride complex is formed in the absence of IL. Surprisingly, in the presence of solely IL (i.e. without hydrogen and carbon dioxide), a hydride peak with low intensity at -19.48 ppm was observed, which suggests that the Ru-cluster may be protonated by residual H_2O. Furthermore, no carbene signal[39] was observed by ^{13}C NMR in any experiment conducted in BMMI.OAc, indicating that there is no interaction between the IL and the Ru-cluster, *via* direct bond formation.
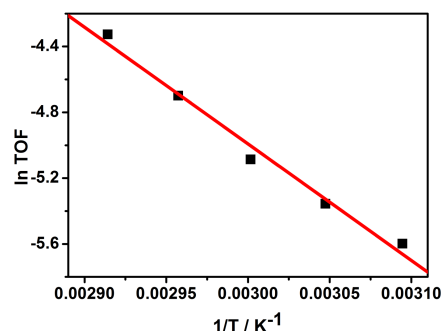
Figure 3. Arrhenius plot for the direct hydrogenation of CO_2 to FA.

The activation barrier for the rate determining step was determined to be 58 kJ mol^{-1} ± 4 kJ mol^{-1}, which is relatively small, given that no electro-donating and/or multidentate ligands have been employed.[14-16, 28b] The range of temperature (50-70 °C) was chosen to avoid catalyst decomposition[41] and side reactions such as the reverse-Water-Gas-Shift reaction at increased temperatures (See SI, Table S4 and Figure 3).[39, 42]

Effect of buffering on FA stabilization

The IL plays an active role in the formation and stabilization of the catalytic active species, and also in the stabilization of the FA via a buffering effect. A linear relationship was found on the double logarithmic scale between the amount of IL present and that of formic acid (Figure 4). This behavior can be explained by the Henderson-Hasselbalch equation typically employed to describe buffering systems. It can be assumed that the IL prevents the deactivation of the

catalyst via protonation by stabilizing the pH at a level that preserves the catalyst in an active state. Another insight that suggests a buffering effect is that a higher acid to buffer ratio can be achieved at low concentrations of buffer (see SI, Figure S3 and Figure S4). A FA/IL ratio of 9:1 was observed at an [IL]=14 mM, which decreased to 3:1 for [IL]=140 mM, reaching a final value of 1.5:1 for [IL]=0.66M (See SI, Figure S3).

Further evidence for the buffering effect is found in the Van't Hoff plot, representing the equilibrium constant at different temperatures (See SI, Table S5 and Figure S5). Values of $\Delta H = -13.26 \pm 0.65$ kJ mol^{-1} and $\Delta S = -17.4 \pm 1.8$ J K^{-1} mol^{-1} were observed. The relatively low values of ΔH suggest that no significant proton abstraction, i.e. formate synthesis, is occurring because as in the presence of bases, the change in enthalpy can be expected to be in the range of -30 kJ mol^{-1} to -84 kJ mol^{-1}.[7] Furthermore, the observed enthalpy change falls in-between that of pure DMSO:water and pure IL, indicating a weak interaction between the IL and the FA, presumably through hydrogen bonding.[29, 31] Also, the relatively low entropic contribution to the reaction (-17.4 $\pm$ 1.8 J K^{-1} mol^{-1}) makes FA the favorable product. The low entropic contribution might be explained by the organization of IL-clusters formed in DMSO, which may form IL-FA adducts due to the augmentation of microstates (entropic driver) imposed by the IL surrounding the catalytically active sites.[43]

The linear behavior of the van't Hoff plot manifests itself in the exponential decay of the FA concentration observed upon increasing the reaction temperature (Figure 4b). For instance, a final concentration of FA of 0.6M can be achieved at 100°C. The concentration increases exponentially when the temperature is successively decreased, reaching 1.1M at 60°C. However, when the temperature is further reduced to 50°C the concentration does not increase, indicating an over-acidification leading to a kinetic deactivation of the catalyst prior to reaching the thermodynamic equilibrium as observed at high pressures (Figure 4b).

The reaction rate was found to be dependent on the total pressure. An increased reaction rate can be observed at increased pressure, which can be explained by the increased concentration of the reagents in the liquid phase (according to Henry's law) and the decreased viscosity of the liquid phase at higher concentrations of dissolved gas (See SI, Figure S6).[44] Furthermore, the increased concentration of CO_2 in the liquid phase might enhance the solubility of H_2, as H_2 is highly soluble in CO_2 which in turn is soluble in the ILs.[45-47] The final concentration obtained at low pressures was found to have a linear relationship with the pressure, in agreement with Henry's law.
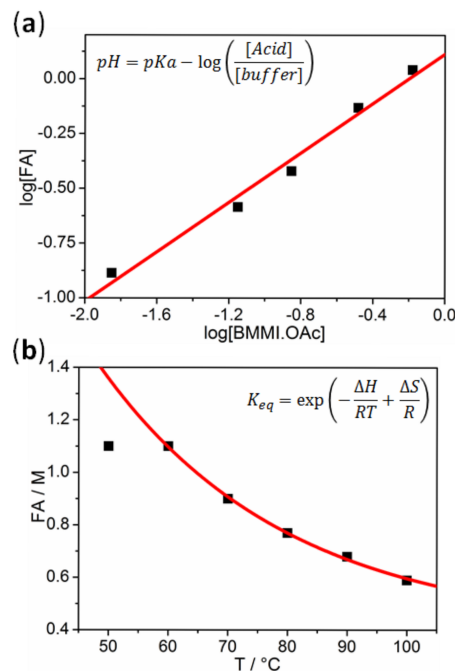
Figure 4. (a) FA concentration vs IL concentration double logarithmic scale. Reaction conditions: $p_{H2} = p_{CO2} = 20$ bar, T = 60°C, 5 mL DMSO:water (5 v/v% water); (b) FA concentration as a function of the temperature of the reaction. Reaction conditions: $p_{H2}=p_{CO2}=20$ bar, 3.3 mmol BMMI.OAc in 5 mL DMSO:water (5 v/v% water).

The favorable thermodynamic parameters in the presence of the IL make the reaction viable at low pressures, where high concentrations of FA (0.47 M) could be observed at low total pressures (6 bar, $p_{H2} = p_{CO2} = 3$ bar). At low pressures, a linear correlation between pressure and concentration of FA was observed, in agreement with Henry's law (Figure 5). This was not the case at higher pressures (>40 bar), potentially due to the catalyst deactivation due to over-acidification of the reaction media or to the saturation of the liquid phase. This is a remarkable result from a processing perspective, since gas compression is the second highest cost after the generation of hydrogen.[48] This suggests that the IL system developed here has extraordinary potential for developing new cost-effective routes towards CO_2 valorization.
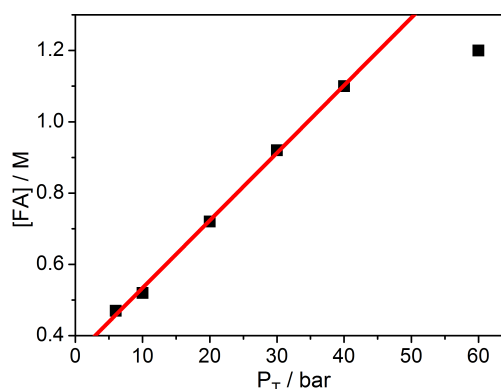
Figure 5. Concentration of FA obtained as a function of the total gas pressure. High concentrations of FA synthesized at low pressures. Reaction conditions: T = 60 °C, 3.3 mmol BMMI.OAc in 5 mL DMSO:water (5 v/v% water).

A critical aspect for the development of viable industrial or commercial processes is the separation of the FA from the IL at the end of the reaction. Our results indicate that the buffering nature of the interaction between FA and the IL, where no formate salts have been formed, should facilitate separation at the end of the synthesis. Nevertheless, it is challenging to separate the liquid FA in a non-energy intensive fashion. Distillation might lead to unwanted dehydration or dehydrogenation reactions[5] and stripping with a carrier solvent, like scCO2, has been shown to have limited efficiency.[31] On the other hand, grafting imidazolium derivatives to commercially available Merrifield resins is a simple strategy to immobilize this type of IL,[49] leading to solid-supported catalysts with analogous properties to homogeneous ILs.[50-52] A similar strategy was employed here, by supporting 1,2-dimethylimidazole onto a microporous Merrifield resin (2 mmol Cl/g, 1% cross-linking) followed by anion exchange to the acetate salt according to literature procedures (see SI for more detail).[53] The supported IL was then employed in place of BMMI.OAc under similar conditions to those previously described. At the end of the reaction the suspension was filtered and characterized by ^{1}H NMR. The polymer was re-utilised in subsequent reaction cycles.

Under optimized conditions (p_{H2} = p_{CO2} = 30 bar, T = 60°C, 0.5 g of polymer, 2 mmol IL-equivalent, 10 mL solvent) a 0.3 M solution of FA (in DMSO/water) was collected by simple filtration, resulting in a FA solution (as shown in Figure 6a) as opposed to the control experiment (Figure 6b), where the employment of a homogeneous ionic liquid lead to a FA-IL mixture. Notably, only traces of FA could be isolated when the reaction was carried out in THF, possibly due to the lower polarity of the solvent leading to a competitive adsorption of the FA on the immobilized IL. This clearly indicates that the reaction is forming formic acid instead of formate adducts with the IL because in the case of formate adduct formation, separation of the formic acid from the IL would be highly unfavorable. Even though the catalyst was only physically adsorbed onto the polymer, the system maintained its activity for five consecutive cycles (see SI, Table S6). Following this, a reduction in activity was observed which was attributed to catalyst leaching. The extent of this was confirmed by ICP-OES analysis of the filtrate which showed significant amounts of ruthenium (Table S6).
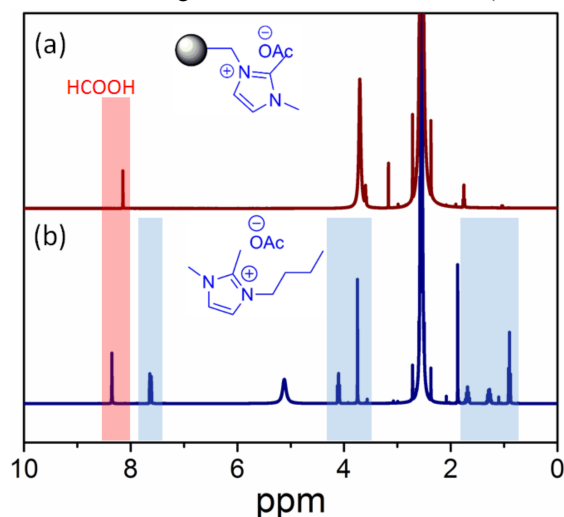
Figure 6. Comparison of the ^{1}H NMR spectra after FA synthesis for: (a) the reaction employing immobilized IL; (b) the reaction employing homogeneous IL.

In addition, the filtrate (FA in the absence of IL) was stable against decomposition. At 60 °C no FA decomposition was observed, even after addition of fresh catalyst (0.016 mmol). Conversely, the FA

decomposition proceeds in the presence of IL at 60 °C, thus indicating that the IL does not only play a role in the formation of formic acid but also in its decomposition (Table S7).

Conclusions

Basic IL are advantageous for the effective hydrogenation of CO_2 under base-free conditions. In this context, the IL plays multiple roles. First, it enhances the catalytic activity of the cheap, simple and readily available [Ru3(CO)12] catalyst by forming intermediate carbonate species which is readily reduced to formic acid. High pressure NMR studies confirmed this and the reaction of CO2 with water containing ILs to form bicarbonate. Furthermore, the IL shifts the equilibrium by acting as a buffer for the acid, thus preventing catalyst deactivation *via* protonation. A profound thermodynamic influence has been observed, where the ionic liquid act as an enthalpic and entropic driver, by structuring the surrounding of the catalyst, thus lowering its contribution and thermodynamically favoring the process.

The finely tuned interaction between the formic acid and the ionic liquid enables the transformation at low pressure and with a broad range of solvents. Besides, it facilitates the separation at the end of the synthesis. A covalently immobilized ionic liquid was found to be as effective as its homogeneous ILs and separation was achieved by simple filtration. Indeed, this represents a major advantage over systems utilizing bases, because reactive distillations could be avoided in future process schemes and thereby enhance the economic viability of sustainable CO_2 valorization.

ASSOCIATED CONTENT

Supporting Information

Experimental details about CO_2 hydrogenation experiments, elucidation of catalytic intermediates, ESI-MS analysis, and thermodynamic parameters calculation. The Supporting Information is available free of charge on the ACS Publications website.

AUTHOR INFORMATION

Corresponding Author

* Jairton.dupont@ufrgs.br
* Victor.sanssangorrin@nottingham.ac.uk

ORCID
Jairton Dupont: 0000-0003-3237-0770
Victor Sans: 0000-0001-7045-5244

Author Contributions

All the authors contributed equally.

REFERENCES

1. Mac Dowell, N.; Fennell, P. S.; Shah, N.; Maitland, G. C., *Nat. Clim. Change* **2017,** 7 (4), 243-249.
2. Reutemann, W.; Kieczka, H. In *Ullmann's Encyclopedia of Industrial Chemistry*, Wiley-VCH Verlag GmbH & Co. KGaA: 2000.

3.	Hull, J. F.; Himeda, Y.; Wang, W.-H.; Hashiguchi, B.; Periana, R.; Szalda, D. J.; Muckerman, J. T.; Fujita, E., *Nat. Chem.* **2012,** *4*, 383-388.
4.	Loges, B.; Boddien, A.; Gärtner, F.; Junge, H.; Beller, M., *Top. Catal.* **2010,** *53*, 902-914.
5.	Grasemann, M.; Laurenczy, G., *Energy Environ. Sci.* **2012,** *5*, 8171-8181.
6.	Leitner, W., *Angew. Chem. Int. Ed. Engl.* **1995,** *34*, 2207-2221.
7.	Schaub, T.; Paciello, R. A., *Angew. Chem. Int. Ed.* **2011,** *50*, 7278-7282.
8.	Inoue, Y.; Izumida, H.; Sasaki, Y.; Hashimoto, H., *Chem. Lett.* **1976,** *5*, 863-864.
9.	Azua, A.; Sanz, S.; Peris, E., *Chem. Eur. J.* **2011,** *17*, 3963-3967.
10.	Sanz, S.; Azua, A.; Peris, E., *Dalton Trans.* **2010,** *39*, 6339-6343.
11.	Himeda, Y.; Onozawa-Komatsuzaki, N.; Sugihara, H.; Kasuga, K., *Organometallics* **2007,** *26*, 702-712.
12.	Himeda, Y.; Miyazawa, S.; Hirose, T., *ChemSusChem* **2011,** *4*, 487-493.
13.	Tanaka, R.; Yamashita, M.; Nozaki, K., *J. Am. Chem. Soc.* **2009,** *131*, 14168-14169.
14.	Filonenko, G. A.; Smykowski, D.; Szyja, B. M.; Li, G.; Szczygieł, J.; Hensen, E. J. M.; Pidko, E. A., *ACS Catal.* **2015,** *5*, 1145-1154.
15.	Filonenko, G. A.; van Putten, R.; Schulpen, E. N.; Hensen, E. J. M.; Pidko, E. A., *ChemCatChem* **2014,** *6*, 1526-1530.
16.	Filonenko, G. A.; Hensen, E. J. M.; Pidko, E. A., *Catal. Sci. Technol.* **2014,** *4*, 3474-3485.
17.	Graf, E.; Leitner, W., *J. Chem. Soc., Chem. Commun.* **1992**, 623-624.
18.	Fornika, R.; Gorls, H.; Seemann, B.; Leitner, W., *J. Chem. Soc., Chem. Commun.* **1995,** 1479-1481.
19.	Elek, J.; Nádasdi, L.; Papp, G.; Laurenczy, G.; Joó, F., *Appl. Catal. A* **2003,** *255*, 59-67.
20.	Tsai, J. C.; Nicholas, K. M., *J. Am. Chem. Soc.* **1992,** *114*, 5117-5124.
21.	Klankermayer, J.; Wesselbaum, S.; Beydoun, K.; Leitner, W., *Angew. Chem. Int. Ed.* **2016,** *55*, 7296-7343.
22.	Wang, W.-H.; Himeda, Y.; Muckerman, J. T.; Manbeck, G. F.; Fujita, E., *Chem. Rev.* **2015,** *115*, 12936-12973.
23.	Dong, K.; Razzaq, R.; Hu, Y.; Ding, K., *Top. Curr. Chem.* **2017,** *375*, 23.
24.	Hayashi, H.; Ogo, S.; Fukuzumi, S., *Chem. Commun.* **2004,** *0*, 2714-2715.
25.	Ogo, S.; Kabe, R.; Hayashi, H.; Harada, R.; Fukuzumi, S., *Dalton Trans.* **2006,** *0*, 4657-4663.
26.	Lu, S.-M.; Wang, Z.; Li, J.; Xiao, J.; Li, C., *Green Chem.* **2016,** *18*, 4553-4558.
27.	Zhao, G.; Joó, F., *Catalysis Commun.* **2011,** *14*, 74-76.
28.	(a) Qadir M. I.; Weilhard, A.; Fernandes, J. A.; de Pedro, I.; Vieira, B.; Waerenborgh, J. C.; Dupont J., *ACS Catal.*, **2018**, DOI: 10.1021/acscatal.7b03804. (b) Moret, S.; Dyson, P. J.; Laurenczy, G., *Nat. Commun.* **2014,** *5*, 4017.
29.	Rohmann, K.; Kothe, J.; Haenel, M. W.; Englert, U.; Hölscher, M.; Leitner, W., *Angew. Chem. Int. Ed.* **2016,** *55*, 8966-8969.
30.	(a) *Cui, G.; Wang, J.; Zhang, S., Chem. Soc. Rev.* **2016**, *45*, 4307-4339. (b) Simon, N. M.; Zanatta, M.; Dos Santos, F. P.; Corvo, M. C.; Cabrita, E. J.; Dupont, J., *ChemSusChem* **2017**, *10*, 4927-4933.
31.	Yasaka, Y.; Wakai, C.; Matubayasi, N.; Nakahara, M., *J. Phys. Chem. A* **2010**, *114*, 3510-3515.
32.	Wesselbaum, S.; Hintermair, U.; Leitner, W., *Angew. Chem.* **2012,** *124*, 8713-8716.
33.	vom Stein, T.; Meuresch, M.; Limper, D.; Schmitz, M.; Hölscher, M.; Coetzee, J.; Cole-Hamilton, D. J.; Klankermayer, J.; Leitner, W., *J. Am. Chem. Soc.* **2014,** *136*, 13217-13225.
34.	Balaraman, E.; Gunanathan, C.; Zhang, J.; Shimon, L. J. W.; Milstein, D., *Nat. Chem.* **2011,** *3*, 609-614.
35.	Burgess, S. A.; Kendall, A. J.; Tyler, D. R.; Linehan, J. C.; Appel, A. M., *ACS Catal.* **2017,** *7*, 3089-3096.
36.	Nevinger, L. R.; Keister, J. B.; Maher, J., *Organometallics* **1990,** *9*, 1900-1905.
37.	Aime, S.; Dastrù, W.; Gobetto, R.; Viale, A., *Organometallics* **1998,** *17*, 3182-3185.
38.	Brewer, S. A.; Holloway, J. H.; Hope, E. G., *J. Fluorine Chem.* **1995,** *70*, 167-169.
39.	Ali, M.; Gual, A.; Ebeling, G.; Dupont, J., *ChemCatChem* **2014,** *6*, 2224-2228.
40.	Ali, M.; Gual, A.; Ebeling, G.; Dupont, J., *ChemSusChem* **2016,** *9*, 2129-2134.
41.	Krämer, J.; Redel, E.; Thomann, R.; Janiak, C., *Organometallics* **2008,** *27*, 1976-1978.
42.	Tominaga, K.-i.; Sasaki, Y.; Hagihara, K.; Watanabe, T.; Saito, M., *Chem. Lett.* **1994,** *23*, 1391-1394.
43.	Luza, L.; Rambor, C. P.; Gual, A.; Bernardi, F.; Domingos, J. B.; Grehl, T.; Brüner, P.; Dupont, J., *ACS Catal.* **2016,** *6*, 6478-6486.
44.	Baker, S. N.; Baker, G. A.; Kane, M. A.; Bright, F. V., *J. Phys. Chem. B* **2001,** *105*, 9663-9668.
45.	Solinas, M.; Pfaltz, A.; Cozzi, P. G.; Leitner, W., *J. Am. Chem. Soc.* **2004,** *126*, 16142-16147.
46.	Blanchard, L. A.; Hancu, D.; Beckman, E. J.; Brennecke, J. F., *Nature* **1999,** *399*, 28-29.
47.	Anthony, J. L.; Maginn, E. J.; Brennecke, J. F., *J. Phys. Chem. B* **2002,** *106*, 7315-7320.
48.	Pérez-Fortes, M.; Schöneberger, J. C.; Boulamanti, A.; Harrison, G.; Tzimas, E., *Int. J. Hydrog. Energy* **2016,** *41*, 16444-16462.
49.	Sans, V.; Karbass, N.; Burguete, M. I.; Compan, V.; Garcia-Verdugo, E.; Luis, S. V.; Pawlak, M., *Chem. Eur. J.* **2011,** *17*, 1894-1906.
50.	Sans, V.; Gelat, F.; Karbass, N.; Burguete, M. I.; Garcia-Verdugo, E.; Luis, S. V., *Adv. Synth. Catal.* **2010,** *352*, 3013-3021.
51.	Burguete, M. I.; Garcia-Verdugo, E.; Garcia-Villar, I.; Gelat, F.; Licence, P.; Luis, S. V.; Sans, V., *J. Catal.* **2010,** *269*, 150-160.
52.	Sans, V.; Gelat, F.; Burguete, M. I.; Garcia-Verdugo, E.; Luis, S. V., *Catal. Today* **2012,** *196*, 137-147.
53.	Burguete, M. I.; Erythropel, H.; Garcia-Verdugo, E.; Luis, S. V.; Sans, V., *Green Chem.* **2008,** *10*, 401-407.